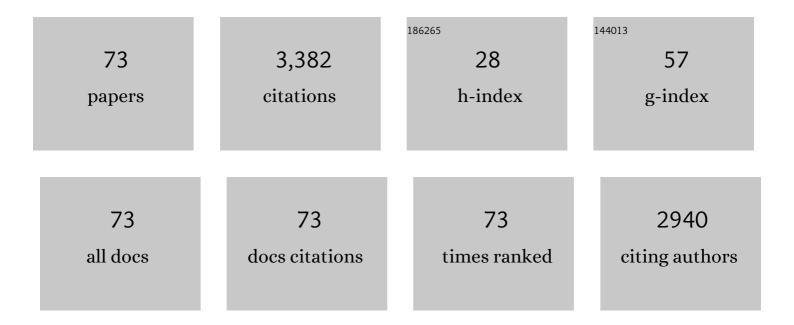
Michel L Schlegel

List of Publications by Year in descending order

Source: https://exaly.com/author-pdf/6560852/publications.pdf Version: 2024-02-01



#	Article	IF	CITATIONS
1	MOX Fuel corrosion processes under waste disposal conditions. Corrosion Science, 2022, 195, 109964.	6.6	1
2	X-ray absorption spectroscopy and actinide electrochemistry: a setup dedicated to radioactive samples applied to neptunium chemistry. Journal of Synchrotron Radiation, 2022, 29, 1-10.	2.4	7
3	Surface Modification of 304L Stainless Steel and Interface Engineering by HiPIMS Pre-Treatment. Coatings, 2022, 12, 727.	2.6	5
4	About the role of iron on the alteration of simplified nuclear glasses in deaerated solutions at 50°C. Journal of Nuclear Materials, 2022, 567, 153820.	2.7	1
5	Investigation of steel corrosion in MX80 bentonite at 120°C. Materials and Corrosion - Werkstoffe Und Korrosion, 2021, 72, 120-130.	1.5	3
6	Mobility of selenium oxyanions in clay-rich media: A combined batch and diffusion experiments and synchrotron-based spectroscopic investigation. Applied Geochemistry, 2021, 128, 104932.	3.0	9
7	Corrosion of carbon steel in clay compact environments at 90 °C: Effect of confined conditions. Corrosion Science, 2021, 184, 109368.	6.6	6
8	Effects of HiPIMS discharges and annealing on Cr-Al-C thin films. Surface and Coatings Technology, 2020, 399, 126141.	4.8	14
9	Corrosion behavior of iron plates in cementitious solution at 80 °C in anaerobic conditions. Corrosion Science, 2020, 170, 108650.	6.6	11
10	Electrochemical and Spectroscopic Study of Eu ^{III} and Eu ^{II} Coordination in the 1â€Ethylâ€3â€methylimidazolium Bis(trifluoromethylsulfonyl)imide Ionic Liquid. Chemistry - A European Journal, 2020, 26, 14385-14396.	3.3	11
11	Long-term corrosion behaviour of carbon steel and stainless steel in Opalinus clay: influence of stepwise temperature increase. Corrosion Engineering Science and Technology, 2019, 54, 516-528.	1.4	4
12	Structural iron in smectites with different charge locations. Physics and Chemistry of Minerals, 2019, 46, 639-661.	0.8	8
13	Corrosion at the carbon steel-clay compact interface at 90°C: Insight into short- and long-term corrosion aspects. Corrosion Science, 2019, 152, 31-44.	6.6	13
14	Electrochemical and Spectroscopic Study of Eu(III)/Eu(II) Couple in the 1-Ethyl-3-Methylimidazolium Bis(Trifluromethanesulfonyl)Imide Ionic Liquid. Minerals, Metals and Materials Series, 2018, , 99-112.	0.4	1
15	Corrosion at the carbon steel-clay borehole water interface under anoxic alkaline and fluctuating temperature conditions. Corrosion Science, 2018, 136, 70-90.	6.6	20
16	Interfacial layers at a nanometre scale on iron corroded in carbonated anoxic environments. RSC Advances, 2017, 7, 20101-20115.	3.6	16
17	Pyrite oxidation in air-equilibrated solutions: An electrochemical study. Chemical Geology, 2017, 470, 67-74.	3.3	23
18	Behavior of heptavalent technetium in concentrated triflic acid under alpha-irradiation: technetium-triflate complex characterized by X-ray absorption fine structure spectroscopy and DFT. Radiochimica Acta, 2017, 105, 135-140.	1.2	5

MICHEL L SCHLEGEL

#	Article	IF	CITATIONS
19	Gaining insight into corrosion processes from numerical simulations of an integrated iron-claystone experiment. Geological Society Special Publication, 2017, 443, 253-267.	1.3	3
20	Corrosion processes of C-steel in long-term repository conditions. Corrosion Engineering Science and Technology, 2017, 52, 127-130.	1.4	12
21	Corrosion processes and microbial activity of carbon steel in the context of geological repository in clay environment. MRS Advances, 2016, 1, 4185-4191.	0.9	2
22	XAS signatures of Am(III) adsorbed onto magnetite and maghemite. Journal of Physics: Conference Series, 2016, 712, 012085.	0.4	7
23	Microstructural characterization of carbon steel corrosion in clay borehole water under anoxic and transient acidic conditions. Corrosion Science, 2016, 109, 126-144.	6.6	28
24	Trivalent Actinide Uptake by Iron (Hydr)oxides. Environmental Science & Technology, 2016, 50, 10428-10436.	10.0	15
25	Alteration of nuclear glass in contact with iron and claystone at 90°C under anoxic conditions: Characterization of the alteration products after two years of interaction. Applied Geochemistry, 2016, 70, 27-42.	3.0	15
26	Corrosion at the carbon steelâ;¿clay borehole water and gas interfaces at 85 °C under anoxic and transient acidic conditions. Corrosion Science, 2016, 111, 242-258.	6.6	35
27	Structural iron in dioctahedral and trioctahedral smectites: a polarized XAS study. Physics and Chemistry of Minerals, 2015, 42, 847-859.	0.8	16
28	Impact of Iron-Reducing Bacteria on the Corrosion Rate of Carbon Steel under Simulated Geological Disposal Conditions. Environmental Science & Technology, 2015, 49, 7483-7490.	10.0	36
29	Oxidative dissolution of iron monosulfide (FeS) in acidic conditions: The effect of solid pretreatment. International Journal of Mineral Processing, 2015, 135, 57-64.	2.6	22
30	Biotic Fe(III) reduction of magnetite coupled to H2 oxidation: Implication for radioactive waste geological disposal. Chemical Geology, 2015, 419, 67-74.	3.3	4
31	Combined geochemical and electrochemical methodology to quantify corrosion of carbon steel by bacterial activity. Bioelectrochemistry, 2014, 97, 61-68.	4.6	20
32	The Oxidative Dissolution of FeS at pH 2.5 in the Presence of Ethylenediaminetetraacetate (EDTA). Procedia Earth and Planetary Science, 2014, 10, 149-153.	0.6	0
33	Behavior of Heptavalent Technetium in Sulfuric Acid under α-Irradiation: Structural Determination of Technetium Sulfate Complexes by X-ray Absorption Spectroscopy and First Principles Calculations. Journal of Physical Chemistry A, 2014, 118, 1568-1575.	2.5	5
34	Carbon steel corrosion in clay-rich environment. Corrosion Science, 2014, 88, 56-65.	6.6	28
35	Corrosion of metal iron in contact with anoxic clay at 90 °C: Characterization of the corrosion products after two years of interaction. Applied Geochemistry, 2014, 51, 1-14.	3.0	51
36	Electrochemical Investigation of the Mechanism of Aqueous Oxidation of Pyrite by Oxygen. Procedia Earth and Planetary Science, 2014, 10, 154-158.	0.6	4

MICHEL L SCHLEGEL

#	Article	IF	CITATIONS
37	Binding mechanism of Cu(II) at the clay–water interface by powder and polarized EXAFS spectroscopy. Geochimica Et Cosmochimica Acta, 2013, 113, 113-124.	3.9	27
38	Dissimilatory Iron Reduction in the Presence of Hydrogen: A Case Study of Microbial Activity and Nuclear Waste Disposal. Procedia Earth and Planetary Science, 2013, 7, 409-412.	0.6	6
39	Effect of Inorganic Anions on FeS Oxidative Dissolution. Procedia Earth and Planetary Science, 2013, 7, 159-162.	0.6	3
40	Reaction of FeS with Fe(III)-bearing acidic solutions. Chemical Geology, 2012, 334, 131-138.	3.3	13
41	In Situ Time-Resolved X-ray Near-Edge Absorption Spectroscopy of Selenite Reduction by Siderite. Environmental Science & Technology, 2012, 46, 10820-10826.	10.0	28
42	Glass–iron–clay interactions in a radioactive waste geological disposal: An integrated laboratory-scale experiment. Applied Geochemistry, 2011, 26, 65-79.	3.0	66
43	Chlorine speciation in nuclear graphite studied by X-ray Absorption Near Edge Structure. Journal of Nuclear Materials, 2011, 418, 16-21.	2.7	10
44	In situ grazing-incidence X-ray diffraction during electrodeposition of birnessite thin films: Identification of solid precursors. Electrochemistry Communications, 2011, 13, 491-494.	4.7	17
45	Influence of exchange correlation on the symmetry and properties of siderite according to density-functional theory. Physical Review B, 2010, 82, .	3.2	16
46	Anodic Activation of Iron Corrosion in Clay Media under Water-Saturated Conditions at 90 °C: Characterization of the Corrosion Interface. Environmental Science & Technology, 2010, 44, 1503-1508.	10.0	77
47	Uptake of uranium and trace elements in pyrite (FeS2) suspensions. Geochimica Et Cosmochimica Acta, 2010, 74, 1551-1562.	3.9	88
48	Sites of Lu(III) Sorbed to and Coprecipitated with Hectorite. Environmental Science & Technology, 2009, 43, 8807-8812.	10.0	22
49	Uranium Uptake by Hectorite and Montmorillonite: A Solution Chemistry and Polarized EXAFS Study. Environmental Science & Technology, 2009, 43, 8593-8598.	10.0	60
50	Oxidation of FeS by oxygen-bearing acidic solutions. Journal of Colloid and Interface Science, 2008, 321, 84-95.	9.4	92
51	Corrosion of iron and low alloyed steel within a water saturated brick of clay under anaerobic deep geological disposal conditions: An integrated experiment. Journal of Nuclear Materials, 2008, 379, 80-90.	2.7	58
52	Diffusion of anionic species in Callovo-Oxfordian argillites and Oxfordian limestones (Meuse/Haute–Marne, France). Applied Geochemistry, 2008, 23, 655-677.	3.0	135
53	Metal corrosion and argillite transformation at the water-saturated, high-temperature iron–clay interface: A microscopic-scale study. Applied Geochemistry, 2008, 23, 2619-2633.	3.0	78
54	Polarized EXAFS characterization of the sorption mechanism of yttrium on hectorite. Radiochimica Acta, 2008, 96, 667-672.	1.2	11

MICHEL L SCHLEGEL

#	Article	IF	CITATIONS
55	Zn Incorporation in Hydroxy-Al- and Keggin Al13-Intercalated Montmorillonite:Â A Powder and Polarized EXAFS Study. Environmental Science & Technology, 2007, 41, 1942-1948.	10.0	26
56	Evidence for the nucleation and epitaxial growth of Zn phyllosilicate on montmorillonite. Geochimica Et Cosmochimica Acta, 2006, 70, 901-917.	3.9	72
57	Cation sorption on the muscovite (001) surface in chloride solutions using high-resolution X-ray reflectivity. Geochimica Et Cosmochimica Acta, 2006, 70, 3549-3565.	3.9	182
58	Molecular environment of iodine in naturally iodinated humic substances: Insight from X-ray absorption spectroscopy. Geochimica Et Cosmochimica Acta, 2006, 70, 5536-5551.	3.9	120
59	Natural speciation of Mn, Ni, and Zn at the micrometer scale in a clayey paddy soil using X-ray fluorescence, absorption, and diffraction. Geochimica Et Cosmochimica Acta, 2005, 69, 4007-4034.	3.9	109
60	Mechanism of Europium Retention by Calcium Silicate Hydrates:Â An EXAFS Study. Environmental Science & Technology, 2004, 38, 4423-4431.	10.0	86
61	Structural evidence for the sorption of Ni(II) atoms on the edges of montmorillonite clay minerals: a polarized X-ray absorption fine structure study. Geochimica Et Cosmochimica Acta, 2003, 67, 1-15.	3.9	109
62	Neoformation of Ni phyllosilicate upon Ni uptake on montmorillonite: A kinetics study by powder and polarized extended X-ray absorption fine structure spectroscopy. Geochimica Et Cosmochimica Acta, 2002, 66, 2335-2347.	3.9	93
63	Structures of quartz (100)- and (101)-water interfaces determined by x-ray reflectivity and atomic force microscopy of natural growth surfaces. Geochimica Et Cosmochimica Acta, 2002, 66, 3037-3054.	3.9	115
64	Sorption of metal ions on clay minerals. III. Nucleation and epitaxial growth of Zn phyllosilicate on the edges of hectorite. Geochimica Et Cosmochimica Acta, 2001, 65, 4155-4170.	3.9	111
65	Adsorption mechanisms of Zn on hectorite as a function of time, pH, and ionic strength. Numerische Mathematik, 2001, 301, 798-830.	1.4	75
66	Molecular-Scale Density Oscillations in Water Adjacent to a Mica Surface. Physical Review Letters, 2001, 87, 156103.	7.8	405
67	Texture effect on polarized EXAFS amplitude. Physics and Chemistry of Minerals, 2001, 28, 52-56.	0.8	33
68	Ni clay neoformation on montmorillonite surface. Journal of Synchrotron Radiation, 2001, 8, 533-535.	2.4	18
69	Crystal chemistry of trace elements in natural and synthetic goethite. Geochimica Et Cosmochimica Acta, 2000, 64, 3643-3661.	3.9	250
70	Sorption of Metal lons on Clay Minerals. Journal of Colloid and Interface Science, 1999, 215, 140-158.	9.4	126
71	Sorption of Metal Ions on Clay Minerals. Journal of Colloid and Interface Science, 1999, 220, 392-405.	9.4	84
72	Evidence for the Formation of Trioctahedral Clay upon Sorption of Co2+ on Quartz. Journal of Colloid and Interface Science, 1999, 220, 181-197.	9.4	80

#	Article	IF	CITATIONS
73	EXAFS Study of Zn and ZnEDTA Sorption at the Goethite (α-FeOOH)/Water Interface. European Physical Journal Special Topics, 1997, 7, C2-823-C2-824.	0.2	20